

On Non-Stationary Urban Macrocell Channels in a Cooperative Downlink Beamforming Scenario

Adrian Ispas and Gerd Ascheid
Institute for Integrated Signal Processing Systems
RWTH Aachen University, Germany
{ispas, ascheid}@iss.rwth-aachen.de

Christian Schneider and Reiner Thomä
Institute of Information Technology
Ilmenau University of Technology, Germany
{christian.schneider, reiner.thomae}@tu-ilmenau.de

Abstract—A common simplification in the treatment of random linear channels is the assumption of stationarity of the channel in time. The wireless channel is, however, known to be inherently non-stationary. We detail a methodology for non-stationarity analysis from an algorithmic perspective. For the determination of local quasi-stationarity regions, we consider a multi-link downlink scenario where multiple base stations use transmit beamforming to concurrently transmit to a single mobile terminal per time slot. We obtain an algorithm-specific measure, i.e., the signal-to-interference-plus-noise ratio (SINR) degradation, with which we evaluate local quasi-stationarity regions. Furthermore, we relate and compare the SINR degradation to the correlation matrix distance (CMD). In an urban macrocell scenario relevant to 3GPP Long Term Evolution (LTE), we find that the resulting local quasi-stationarity distances show the same trends, but that the CMD overestimates the average distances for our system model.

I. INTRODUCTION

Due to its complexity, the wireless channel is typically treated as a random (linear) channel with the additional assumption of stationarity in time. However, the wireless channel is known to be inherently non-stationary [1]. As several algorithms in digital communications rely on the stationarity of the channel, a practical approach is to define local quasi-stationarity regions [2], i.e., local regions in which a stochastic process is approximated as stationary. Inside these regions, the algorithms operate with constant statistical knowledge.

Several different measures have been proposed in the literature to characterize the non-stationarity of the channel, the most famous regarding spatial channel properties is the correlation matrix distance (CMD). However, they mostly focus on, to some extent, arbitrary properties of the channel. From the point of view of an algorithm, only some specific properties of the channel are important. This could, e.g., be a subset of the information given by second order moments of the channel process. First attempts to relate the non-stationarity analysis to an algorithmic view are done in [3] and [4]. In [3], a multiple-input and multiple-output (MIMO) prefiltering technique is used to simulatively compare the performance, more specifically the bit error rate (BER), results to the CMD results in an indoor scenario. However, this approach does not give an analytical connection between the measure and the algorithm. In [5], measures related to a prediction and interpolation algorithm are derived to compare power spectral densities (PSDs) of stationary processes. In [4], one of these

measures has been applied to the characterization of non-stationary channels. The considered algorithms have, however, simplifying assumptions, e.g., noiseless observations.

We detail a methodology to determine local quasi-stationarity regions from a realistic algorithmic perspective, as in the end one is interested in the performance, or more exactly the performance degradation due to mismatched statistics of the channel, of a particular algorithm. This is the quantity that is relevant to define local quasi-stationarity regions since it gives the regions in which the statistical information about the channel can be kept constant for the algorithm.

Contribution: We analyze the non-stationarity of the wireless channel in a scenario with cooperative base stations (BSs) performing downlink beamforming to a single mobile terminal (MT) per time slot over a flat-fading multiple-input and single-output (MISO) channel. The measurements are performed in an urban macrocell scenario relevant to 3GPP Long Term Evolution (LTE). In particular, we contribute

- an algorithm-specific measure for non-stationarity analysis, i.e., the signal-to-noise-plus-interference ratio (SINR) degradation,
- a relation of the SINR degradation to the (TX) CMD,
- an evaluation and comparison of local quasi-stationarity regions based on the SINR degradation and the TX CMD.

Notation: \mathbf{A}^* , \mathbf{A}^T , and \mathbf{A}^H denote the (element-wise) complex conjugate, the transpose, and the conjugate transpose of the matrix \mathbf{A} , respectively. $\text{tr}\{\mathbf{A}\}$ and $\|\mathbf{A}\|_F$ denote the trace and the Frobenius norm of the matrix \mathbf{A} , respectively. $\mathbf{A} \oplus \mathbf{B}$ denotes the block matrix resulting from the direct sum of the matrices \mathbf{A} and \mathbf{B} . $[\mathbf{A}]_{i,j}$ denotes the element in the i -th row and j -th column of \mathbf{A} . $|\mathcal{A}|$ denotes the cardinality of the set \mathcal{A} . $\delta[k,l]$ denotes the 2-dimensional Kronecker delta.

II. SYSTEM MODEL

We consider a multi-link downlink scenario where multiple BSs concurrently transmit to a single MT per time slot. The BSs use local statistical knowledge about the channel, i.e., each BS has only statistical channel knowledge about its own link to the MT, to perform transmit beamforming. Furthermore, we assume that transmission is taking place over a random, time-varying, and flat-fading¹ MISO channel with

¹In a cyclic prefix-based OFDM setting for delay-underspread channels, our approach corresponds to a per carrier treatment.

N_a antennas at each BS and a single antenna at the MT. We assume to have perfect timing synchronization from the BSs to the MT. In the complex baseband, the matched-filtered, symbol-sampled (discrete-time) received signal at the MT is given by

$$y[m] = \sum_{k=1}^{N_{BS}} \mathbf{L}_{H,k}[m] \mathbf{w}_k[m] x[m] + n[m] \quad (1)$$

where k denotes the considered BS and N_{BS} denotes the number of BSs. $\mathbf{L}_{H,k}[m]$ is a row vector containing the (random) time-varying and frequency-constant channel transfer functions of the sub-links from the individual antennas of BS k to the MT. We assume $\mathbf{L}_{H,k}[m]$ as independent across links from the different BSs k to the MT. $\mathbf{w}_k[m]$ are the (deterministic) beamforming weights of BS k normalized to $\mathbf{w}_k^H[m] \mathbf{w}_k[m] = 1$, $x[m]$ is the (random) signal transmitted from the BSs with power $\mathbb{E}\{|x[m]|^2\} = \sigma_x^2$, and $n[m]$ denotes combined interference (from outside our scenario) and receiver noise with power $\sigma_n^2[m]$.

A. Beamforming Technique

In order to allow an intuitive, yet realistic analysis of the non-stationarity of the channel, we choose the so-called eigenbeamforming technique, i.e., we use the (element-wise) complex conjugate of the dominant eigenvectors² of the channel correlation matrices as the beamforming weights. Assuming only (local) knowledge of the channel correlation matrices at the transmitting BSs, this technique maximizes the SINR at the receiving MT for our system model. In mathematical terms, we have

$$\mathbf{w}_k[m] = \mathbf{u}_{max,k}^*[m] \quad (2)$$

where $\mathbf{u}_{max,k}[m]$ is the dominant eigenvector of $\mathbf{R}_k[m]$ and

$$\mathbf{R}_k[m] \triangleq \mathbb{E}\{\mathbf{L}_{H,k}^T[m] \mathbf{L}_{H,k}[m]\} \quad (3)$$

is the (Hermitian and positive semidefinite) correlation matrix of the channel for the link from BS k to the MT.

III. SINR DEGRADATION

Based on our system model, our goal is to use a meaningful measure to analyze the non-stationarity of the channel. Concretely, we define local quasi-stationarity regions of the channel based on the degradation of the system performance. In our scenario, the SINR at the MT is a meaningful measure to characterize the system performance and, thus, we look at the degradation of the SINR due to changes in the statistics of the channel.

The mismatched SINR at time instant m using knowledge of the channel correlation matrix at time instant m' is

$$SINR[m, m'] = \frac{\sum_{k=1}^{N_{BS}} \mathbf{w}_k^T[m'] \mathbf{R}_k[m] \mathbf{w}_k^*[m']}{\sigma_n^2[m] / \sigma_x^2} \quad (4)$$

$$= \frac{\sum_{k=1}^{N_{BS}} \mathbf{u}_{max,k}^H[m'] \mathbf{R}_k[m] \mathbf{u}_{max,k}[m']}{\sigma_n^2[m] / \sigma_x^2}. \quad (5)$$

²The dominant eigenvector of a matrix \mathbf{A} is the eigenvector of \mathbf{A} corresponding to the maximal eigenvalue of \mathbf{A} .

In the optimal case, we have $m' = m$. The SINR degradation is defined as

$$\begin{aligned} SINR_{deg}[m, m'] &\triangleq 1 - \frac{SINR[m, m']}{SINR[m, m]} \\ &= 1 - \frac{\sum_{k=1}^{N_{BS}} \mathbf{u}_{max,k}^H[m'] \mathbf{R}_k[m] \mathbf{u}_{max,k}[m']}{\sum_{k=1}^{N_{BS}} \lambda_{max,k}[m]}. \end{aligned} \quad (6)$$

Note that only changes in second order moments of the channel are characterized by the SINR degradation.

A. Relation to the CMD for $N_{BS} = 1$

In [6], the CMD has been proposed to characterize the non-stationarity of single link MIMO channels. Essentially, the CMD in time characterizes the (dis)similarity in time of the spatial properties only of the MIMO channel. For our MISO channel with $N_{BS} = 1$, only the spatial transmitter (TX) properties at one BS are relevant. We, thus, use the TX CMD defined as

$$CMD_{TX}[m, m'] \triangleq 1 - \frac{\text{tr}\{\mathbf{R}[m] \mathbf{R}[m']\}}{\|\mathbf{R}[m]\|_F \|\mathbf{R}[m']\|_F}. \quad (7)$$

Furthermore, using the eigendecomposition of a Hermitian matrix $\mathbf{R} = \mathbf{U} \mathbf{\Lambda} \mathbf{U}^H$, with the real and non-negative eigenvalue $\lambda_i[m] = [\mathbf{\Lambda}[m]]_{i,i}$ and the eigenvector $\mathbf{u}_i[m]$ being the i -th column of $\mathbf{U}[m]$, we have

$$\begin{aligned} \text{tr}\{\mathbf{R}[m] \mathbf{R}[m']\} &= \text{tr}\{\mathbf{R}[m] \mathbf{U}[m'] \mathbf{\Lambda}[m'] \mathbf{U}^H[m']\} \\ &= \text{tr}\{\mathbf{U}^H[m'] \mathbf{R}[m] \mathbf{U}[m'] \mathbf{\Lambda}[m']\} \\ &= \text{tr}\left\{\mathbf{U}^H[m'] \mathbf{R}[m] \mathbf{U}[m'] \sum_i \lambda_i[m'] \mathbf{J}^{ii}\right\} \\ &= \sum_{i=1}^{N_a} \lambda_i[m'] [\mathbf{U}^H[m'] \mathbf{R}[m] \mathbf{U}[m']]_{i,i} \\ &= \sum_{i=1}^{N_a} \lambda_i[m'] \mathbf{u}_i^H[m'] \mathbf{R}[m] \mathbf{u}_i[m'] \end{aligned} \quad (8)$$

where the single-entry matrix \mathbf{J}^{ii} is defined by $[\mathbf{J}^{ij}]_{k,l} \triangleq \delta[k-i, l-j]$. With (8), we can rewrite (7) as

$$CMD_{TX}[m, m'] = 1 - \frac{\sum_{i=1}^{N_a} \lambda_i[m'] \mathbf{u}_i^H[m'] \mathbf{R}[m] \mathbf{u}_i[m']}{\sqrt{\sum_{i=1}^{N_a} \lambda_i^2[m] \sum_{i=1}^{N_a} \lambda_i^2[m']}}. \quad (9)$$

When $\mathbf{R}[m]$ and $\mathbf{R}[m']$ have only one positive (strictly larger than 0) eigenvalue each, i.e., they are rank 1 matrices, then the TX CMD and the SINR degradation reduce to an identical measure. This shows that there is a clear connection between the two measures, and, in some sense, can justify the use of the CMD for the characterization of the non-stationarity of the channel w.r.t the system performance of our beamforming technique. Note that the subsequent analysis is not restricted to rank 1 matrices.

For the multi-BS MISO channel considered here, one could extend the TX CMD using $\mathbf{R}_{ext}[m] \triangleq \mathbf{R}_1[m] \oplus \dots \oplus \mathbf{R}_{N_{BS}}[m]$ instead of $\mathbf{R}[m]$ since the links are assumed to be independent. This extended TX CMD reduces to the (classical) TX CMD in

the single BS case, i.e., for $N_{BS} = 1$. However, due to space constraints, it is not further considered in this work.

B. Local Quasi-Stationarity

Defining sets $\mathcal{M}_j[m]$ using thresholds th_j as

$$\mathcal{M}_{SINR}[m] \triangleq \{m' \mid SINR_{deg}[m, m'] < th_{SINR}\} \quad (10)$$

$$\mathcal{M}_{CMD}[m] \triangleq \{m' \mid CMD_{TX}[m, m'] < th_{CMD}\} \quad (11)$$

we obtain time-dependent local quasi-stationarity times

$$T_{stat,j}[m] \triangleq |C_j[m]| T_s \quad (12)$$

where $C_j[m]$ is the connected subset of $\mathcal{M}_j[m]$ with maximum cardinality and containing m . Generally, thresholds and, thus, the local quasi-stationarity times depend on the accuracy that is required for the considered algorithm.

IV. MEASUREMENT CAMPAIGN

Our MIMO channel measurement campaign focuses on gathering realistic channel data in an urban macrocell scenario relevant to 3GPP LTE. Channel sounding is conducted at 2.53 GHz in 2 bands of 45 MHz.

On the BS side, a uniform linear array (ULA) with 8 dual-polarized (horizontally and vertically) elements is used. Each element consists of a stack of 4 patches in order to form a narrow transmit beam in elevation. At the MT (passenger car) a uniform circular array (UCA) with 2 rings of 12 dual-polarized patches is used. Additionally, a cube with 5 patches is placed on top. The BS serves as the TX and the MT as the receiver (RX).

The measurement campaign sequentially covers 3 BS positions with 25 m, 15 m, and 3.5 m height, and a centrally located relay point with 3.5 m height. In total 22 individual MT tracks with more than 120 measurement runs are performed. In Fig. 1, an overview of the 3 MT reference tracks and the 3 BS positions is shown. A distinction between line-of-sight (LOS) and non-LOS (NLOS) situations is made possible by the use of ray tracing data.

Table I summarizes the properties of the measurement campaign. For further details, we refer to [7], [8], and [9].

V. DATA PROCESSING

For the characterization, we choose the BS ULA on the 3 BS positions at a height of 25 m as the TX array, and the lower MT UCA on the 3 MT reference tracks as the RX array. We use a 20 MHz band³ between 2.49 GHz and 2.51 GHz and study vertically polarized propagation. The considered MISO link consists of the central 4 antenna elements at the BS (TX) and 1 antenna element per orientation at the MT (RX). The 4 orientations are the front (direction of motion), the back, and the 2 sides of the MT. We preprocess the data by estimating a noise level in the time-delay domain and not considering any values below it.

In order to estimate the correlation matrices, we want to approximate the ensemble averaging by an averaging operation

³Note that the bandwidth chosen here is only used for data processing, i.e., it is not equal to the transmission bandwidth in our system model.

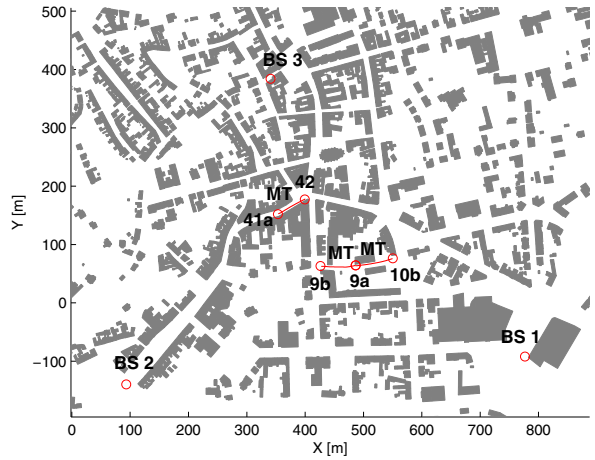


Fig. 1. Overview of the MT reference tracks and the 3 BS positions

over time and frequency. However, before doing so, we verify the doubly underspread (DU) assumption $\Delta\tau_{max}\Delta\nu_{max} \ll \tau_{max}\nu_{max} \ll 1$ to guarantee that an averaging over time and frequency is meaningful [10]. In [1], we showed that in our scenario the DU assumption is fulfilled with $\Delta\tau_{max}\Delta\nu_{max} \approx 1.16 \cdot 10^{-7}$ and $\tau_{max}\nu_{max} \approx 1.17 \cdot 10^{-4}$. Furthermore, we showed that here an averaging in time over $N_t = 16$ and in frequency over $N_f = 128$ samples is a sensible choice to study local quasi-stationarity in time. In total we, thus, average over

GENERAL PROPERTIES		
Scenario	Urban macrocell	
Location	City center, Ilmenau, Germany	
MIMO measurement setup	3 BSs, 1 relay station, 22 tracks	
Intersite distances	BS 1-2: 680 m	
	BS 2-3: 580 m	
	BS 3-1: 640 m	
CHANNEL SOUNDER PROPERTIES		
Type	RUSK TUI-FAU, Medav GmbH	
TX power	46 dBm at the power amplifier output	
Center frequency f_c	2.53 GHz	
Bandwidth	2 bands of 45 MHz	
Time sample spacing T_s	13.1 ms	
Frequency sample spacing F_s	156.25 kHz	
MIMO sublinks	928 ($N_{TX} = 16$, $N_{RX} = 58$)	
AGC switching	In MIMO sublinks	
Positioning	Odometer and GPS	
ANTENNA PROPERTIES		
	TX array	RX array
Type	PULPA8	SPUCPA 2x12 + cube
Height	25 m, 15 m, 3.5 m	1.9 m
Beamwidth, azimuth (3dB)	100°	360°
Beamwidth, elevation (3dB)	24°	80°
Tilt	5° down	0
Maximal velocity $ v_{max} $	0	≈ 10 km/h

TABLE I
PROPERTIES OF THE MEASUREMENT CAMPAIGN

2048 (≈ 500 non-coherent, see [1]) realizations. This should be sufficient for an accurate estimation; however, no claims of optimality are made for these parameters.

The results on the local quasi-stationarity in time are mapped to the driven distance using the positioning information obtained during the measurement campaign. Assuming that only the MT is moving, i.e., scatterers and the currently used BS are fixed, this gives a representation of the local quasi-stationarity in distance at the MT.

Since the measurements were performed sequentially for each combination of BS and MT track, the positions of the measurements from the different BSs to one track are matched to reduce positioning errors of the different measurements runs. Obviously, this matching process is bound to contain errors as a perfect rerun of the tracks is not possible.

VI. RESULTS OF THE DATA ANALYSIS

First, we extract LOS/NLOS information from ray tracing data. We find that LOS occurs for the link from BS 1 to track 10b-9a up to a distance of approx. 25 m, for the link from BS 2 to track 10b-9a starting at a distance of approx. 5 m up to the end, and for the link from BS 2 to track 9a-9b from the beginning to approx. 5.5 m and from approx. 50.5 m to the end. The remaining measurements (of the 3 BS and the 3 reference tracks) covered NLOS situations.

For the subsequent analysis, we choose a threshold $th_{SINR} = 0.1$, i.e., we define a 10% degradation or approx. a 0.46 dB loss of the received SINR (due to mismatched statistical knowledge) to be the minimal loss that is not acceptable anymore. Thus, according to our definition, for an SINR degradation that is equal or higher than this threshold, local quasi-stationarity is not fulfilled anymore. Exemplarily, we focus our analysis on track 10b-9a, since this track features LOS and NLOS situations. Fig. 2 shows the received SINR in the optimal case ($m' = m$) for track 10b-9a and the 4 orientations (with $\sigma_n^2[m]/\sigma_x^2 = 1$). One can see that, especially for the left direction, a high SINR is seen for the link from BS 1 up to approx. 25 m. This corresponds exactly to the LOS part. However, we cannot see a significant influence of the LOS part from BS 2, as it covers almost the whole track. Due to the larger distance of BS 2 from track 10b-9a (approx. 505 m to 443 m) and, thus, a high path loss, the SINR is relatively low. The SINR of the cooperative scheme using all BSs, i.e., the sum of the individual SINRs of the BSs is also shown. In the beginning part of the track, the contribution from BS 1 is seen to be dominant. This is due to LOS, on the one hand, and to the shorter distance to BS 1 (approx. 283 m to 330 m), on the other hand. However, towards the end of the track, BS 3 (approx. 372 m to 351 m) contributes significantly to the total SINR as a strong reflection is expected from the left. Using all links, i.e., all combinations of BSs and MT tracks, and all 4 orientations, in Fig. 3, we show a histogram of the (optimal) gain of the cooperative scheme compared to the individual scheme with the highest SINR. One can see that the SINR gain compared to the strongest link is usually rather low, in fact an SINR gain of 2 (approx. 3 dB) or more

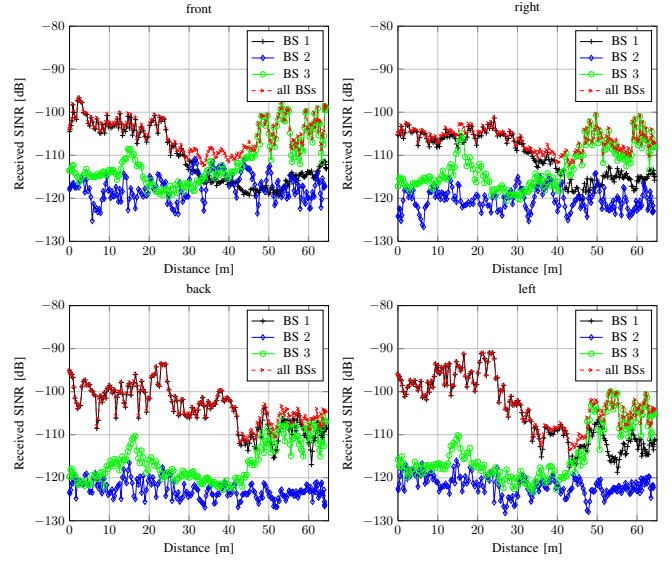


Fig. 2. Received SINRs in the optimal case for track 10b-9a

is only obtained in approx. 5.7 % of the cases. This is due to the presence of single dominant links with, e.g., LOS.

Fig. 4 depicts the local quasi-stationarity distances using the SINR degradation which result from (12) with (10). Due to clarity of exposition, we only show the resulting distances for BS 1 and the cooperative scheme. They exhibit strong variations, but the resulting distances for the left orientation show a strong and constant peak at the beginning of the track for both cases. It coincides with the LOS part from BS 1 that is relevant for the left orientation.

In Table II, the average local quasi-stationarity distances $\bar{d}_{stat,SINR}$ are given for all schemes, BSs, MT tracks, and orientations. In general, the cooperative scheme using all BSs shows average distances in-between the minimal and the maximal value of the ones from the individual schemes using BS 1, BS 2, and BS 3 separately. Furthermore, the link from BS 2 to track 10b-9a has high average distances for the back and the left orientations. As mentioned before, this link features LOS for almost the whole track, and, thus, slowly varying propagation conditions can be expected.

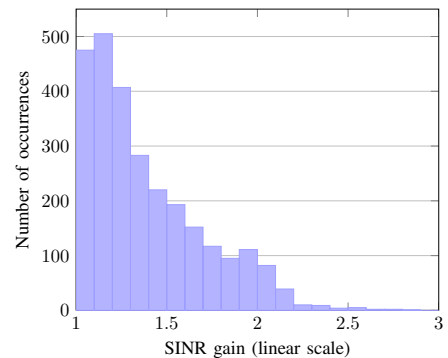


Fig. 3. Histogram of the (optimal) cooperative SINR gain using all links and all orientations

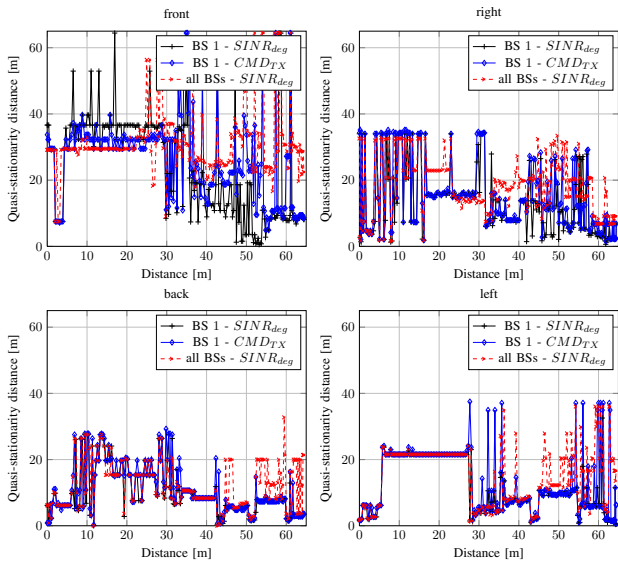


Fig. 4. Local quasi-stationarity distances for track 10b-9a

A. Comparison to the CMD for BS 1

We now restrict our analysis to the case $N_{BS} = 1$. In particular, we look at the links from BS 1 to the 3 reference tracks. In order to allow for a fair comparison between the SINR degradation and the TX CMD, we choose the same thresholds, i.e., $th_{CMD} = th_{SINR} = 0.1$. Exemplarily, in Fig. 4, we depict the evolution over time of the local quasi-stationarity distances using the TX CMD, resulting from (12) with (11), for track 10b-9a. We observe strong similarities between the two measures. Further, comparing the results of the average local quasi-stationarity distances using the SINR degradation $\bar{d}_{stat,SINR}$ for BS 1 in Table II to the corresponding results for the TX CMD $\bar{d}_{stat,CMD}$ in Table III, we can confirm that the resulting average distances show the same trends. However, the average distances obtained using the TX CMD are higher, i.e., the TX CMD overestimates the average local quasi-stationarity distances w.r.t. our system model. Thus, the TX CMD gives some indication about the

BS	Track	$\bar{d}_{stat,SINR}$ per orientation [m]			
		front	right	back	left
1	10b-9a	23.10	12.93	9.58	10.88
	9a-9b	36.30	30.87	3.86	8.67
	41a-42	50.97	51.04	28.92	31.74
2	10b-9a	22.74	40.93	64.04	60.66
	9a-9b	7.39	16.28	57.99	55.01
	41a-42	52.71	52.71	45.95	50.47
3	10b-9a	24.14	22.59	10.52	13.11
	9a-9b	31.69	23.89	29.17	24.99
	41a-42	8.58	10.85	11.97	25.10
all	10b-9a	31.14	17.89	12.35	15.10
	9a-9b	21.48	23.96	16.53	23.64
	41a-42	15.28	16.33	21.92	30.75

TABLE II

AVERAGE LOCAL QUASI-STATIONARITY DISTANCES USING $SINR_{deg}$

BS	Track	$\bar{d}_{stat,CMD}$ per orientation [m]			
		front	right	back	left
1	10b-9a	25.55	15.34	10.38	13.02
	9a-9b	38.50	39.13	6.94	11.24
	41a-42	51.23	51.97	30.86	33.61

TABLE III

AVERAGE LOCAL QUASI-STATIONARITY DISTANCES USING CMD_{TX}

size of local quasi-stationarity regions, but a correct approach regarding system performance requires an algorithm-specific measure, e.g., the SINR degradation given in (6).

VII. CONCLUSION

In this work, we detailed a methodology to analyze non-stationarity from a realistic algorithmic perspective. For the determination of local quasi-stationarity regions, we considered a multi-link downlink scenario where multiple BSs use transmit beamforming to concurrently transmit to a single MT per time slot. We obtained an algorithm-specific measure, i.e., the SINR degradation, with which we evaluated local quasi-stationarity regions in an urban macrocell scenario relevant to 3GPP LTE. Furthermore, we related the SINR degradation to the (TX) CMD and compared their results. Even though, SINR degradation and TX CMD differ, we found strong similarities between the local quasi-stationarity distances based on these measures. However, the TX CMD overestimates the average local quasi-stationarity distances w.r.t. our system model. The, on average, relatively high local quasi-stationarity distances for an acceptable SINR degradation of 10% suggest the possibility of a low update rate of the channel statistics for beamforming techniques as the one considered here.

REFERENCES

- [1] A. Ispas, C. Schneider, G. Ascheid, and R. Thomä, "Analysis of local quasi-stationarity regions in an urban macrocell scenario," in *Proc. 71st IEEE Vehicular Technology Conference (VTC 2010-Spring)*, Taipei, Taiwan, May 2010.
- [2] P. Bello, "Characterization of randomly time-variant linear channels," *IEEE Trans. Commun.*, vol. 11, no. 4, pp. 360–393, Dec. 1963.
- [3] M. Herdin, N. Czink, H. Özcelik, and E. Bonek, "Correlation matrix distance, a meaningful measure for evaluation of non-stationary MIMO channels," in *Proc. 61st IEEE Vehicular Technology Conference (VTC 2005-Spring)*, vol. 1, Stockholm, Sweden, Jun. 2005, pp. 136–140.
- [4] L. Bernadó *et al.*, "Non-WSSUS vehicular channel characterization at 5.2 GHz - Spectral divergence and time-variant coherence parameters," in *Proc. XXIXth URSI General Assembly*, Chicago, IL, USA, Aug. 2008.
- [5] T. T. Georgiou, "Distances and Riemannian metrics for spectral density functions," *IEEE Trans. Signal Process.*, vol. 55, no. 8, pp. 3995–4003, Aug. 2007.
- [6] M. Herdin and E. Bonek, "A MIMO correlation matrix based metric for characterizing non-stationarity," in *Proc. IST Mobile and Wireless Communications Summit (ICT-MobileSummit 2004)*, Lyon, France, Jun. 2004.
- [7] C. Schneider *et al.*, "Multi-user MIMO channel reference data for channel modelling and system evaluation from measurements," in *Proc. Int. ITG Workshop on Smart Antennas (WSA 2009)*, Berlin, Germany, Feb. 2009.
- [8] R. S. Thomä, D. Hampicke, A. Richter, G. Sommerkorn, and U. Trautwein, "MIMO vector channel sounder measurement for smart antenna system evaluation," *European Transactions on Telecommunications*, vol. 12, no. 5, pp. 427–438, Sep.-Oct. 2001.
- [9] Institute of Information Technology, Ilmenau University of Technology. (2009, Apr.) Ilmenau reference scenario. [Online]. Available: <http://www-emt.tu-ilmenau.de/ReferenceScenario/>
- [10] G. Matz, "On non-WSSUS wireless fading channels," *IEEE Trans. Wireless Commun.*, vol. 4, no. 5, pp. 2465–2478, Sep. 2005.